Transplant Immunology 52 (2019) 57–67

Contents lists available at ScienceDirect

Transplant Immunology

journal homepage: www.elsevier.com/locate/trim

Regulatory effects of dermal papillary pluripotent stem cells on polarization of macrophages from M1 to M2 phenotype in vitro

Meiying Li[a,b,*,1], Jiayi Xu[a,c,1], Xianglin Mei[d,e], Guangfan Chi[a], Lisha Li[a], Yaolin Song[a], Xia He[a], Yulin Li[a,*]

[a] The Key Laboratory of Pathobiology, Ministry of Education, Jilin University, Changchun, Jilin 130021, PR China
[b] Department of Surgery, The First Hospital of Jilin University, Changchun, Jilin 130021, PR China
[c] Department of Pathology, Central Hospital of Panzhihua, Panzhihua, Sichuan 617067, PR China
[d] Department of Pathology, Second Hospital of Jilin University, Changchun, Jilin 130000, PR China
[e] National Engineering Laboratory for Druggable Gene and Protein Screening, Northeast Normal University, Changchun, Jilin 130024, PR China

ARTICLE INFO

Keywords:
Spinal cord injury
Macrophage
Polarization
Dermal papilla cell
Mesenchymal stem cell

ABSTRACT

The M1:M2 macrophage ratio is important for spinal cord injury (SCI) repair. Bone marrow mesenchymal stem cells (BMSCs) can alter macrophage activation, promoting M1 to M2 macrophage conversion and SCI repair; however, clinical BMSC applications have limitations. Previously, we found DPCs to be superior to BMSCs in promoting tissue repair after SCI, which we hypothesized to be mediated by M1 to M2 macrophage conversion. We investigated the regulatory effect of DPCs on M1/M2 macrophage polarization. Dermal papilla cells (DPCs) were isolated from rat vibrissae and characterized. Bone marrow-derived macrophages (BMDMs) were isolated and identified based on specific marker expression, and stimulated to differentiate into M1 macrophages with GM-CSF, IFN-γ, and LPS. These cells were co-cultured with DPCs to evaluate the effect on macrophage differentiation. DPCs expressed dermal papillae-specific markers, including ALP and Sox2, had MSC-expression patterns like those of BMSCs, and were capable of multi-differentiation. BMDMs expressed ANAE and CD68. Three days after induction, differentiated cells exhibited morphology typical of M1-like macrophages and expressed the macrophage marker CD68 and the M1 macrophage markers iNOS, but lacked expression of the M2 macrophage marker CD206. Co-culture with DPCs resulted in a shift to anti-inflammatory M2-like macrophage differentiation, characterized by morphological changes typical of M2 macrophages, downregulation of the characteristic cytokine TNF-α and the proportion of $iNOS^+$ cells, and upregulation of the characteristic cytokine IL-10 and the cell-surface marker CD206. The number of CD206-expressing M2 macrophages also increased. These findings demonstrate that DPCs reprogram macrophages to an anti-inflammatory M2 phenotype, which could improve adverse inflammatory microenvironments and promote tissue repair. Thus, DPCs may be an interesting alternative cell source and merit further investigation in applications for SCI therapy.

1. Introduction

To treat spinal cord injury (SCI), it is important to not only replenish/replace damaged necrotic neurons/glial cells, but also to improve the associated adverse inflammatory microenvironment [1]. Transplantation of stem cells (such as embryonic, inducible pluripotent, neural, and neural crest stem cells) constitutes a promising therapeutic option for SCI; however, despite its theoretical benefits, many issues remain regarding the use of stem cells for this application. For example, although stem cells can differentiate into neurons/glial cells to replace

List of Abbreviations: ALP, alkaline phosphatase; ANAE, α-naphthyl acetate esterase; Arg1, arginase-1; BDNF, brain-derived neurotrophic factor; BMDM, bone marrow-derived macrophage; BMSC, bone marrow mesenchymal cell; DMEM, Dulbecco's modified Eagle's medium; DPC, dermal papilla cell; FBS, fetal bovine serum; GM-CSF, granulocyte macrophage-colony stimulating factor; IFN, interferon; IL, interleukin; iNOS, inducible nitric oxide synthase; LPS, lipopolysaccharide; MSC, mesenchymal stem cell; PBS, phosphate buffered saline; RT-PCR, reverse-transcription-polymerase chain reaction; qPCR, real time quantitative polymerase chain reaction; SCI, spinal cord injury; TrkB, tropomyosin-related kinase B; TGF-β, transforming growth factor beta; TNF-α, tumor necrosis factor-alpha; VEGF, vascular endothelial growth factor

* Correspondence authors at: The Key Laboratory of Pathobiology, Ministry of Education, Jilin University, 126 Xinmin Street, Changchun, Jilin 130021, PR China.
E-mail addresses: limeiying@jlu.edu.cn (M. Li), ylli@jlu.edu.cn (Y. Li).
[1] Contributed equally.

https://doi.org/10.1016/j.trim.2018.11.003
Received 27 August 2018; Received in revised form 14 November 2018; Accepted 16 November 2018
Available online 17 November 2018
0966-3274/

the corresponding damaged cells in the host [2], acute inflammation following SCI often leads to the death of transplanted cells, which comprises the main barrier for efficient cell-transplant therapy in early SCI (1–7 days after injury) [3]. In addition, the occurrence of an inflammatory response can also result in the death of a wide range of neurons and microglial cells, axial mutation, and glial scar formation, in turn causing further tissue damage. Conversely, macrophage phagocytosis during inflammation is also beneficial for the recovery of nerve regeneration and function. As such, macrophage polarization plays an important role in SCI and damage repair mediated by the inflammatory response [4,5].

The term “polarization” refers to the phenomenon by which macrophages can exhibit different functional phenotypes in different microenvironments. This mainly includes “classic activated macrophages” (M1, pro-inflammatory) and “alternative activated macrophages” (M2, anti-inflammatory) [6]. Macrophages can be induced to become M1 macrophages through culture with a combination of lipopolysaccharide (LPS), interferon gamma (IFN-γ), and granulocyte macrophage-colony stimulating factor (GM-CSF). These cells are characterized by the secretion of high levels of interleukin-1 beta (IL-1β), IL-6, IL-12, tumor necrosis factor-alpha (TNF-α), IFN-γ, and other pro-inflammatory factors. During the secondary SCI stage, M1-type macrophages mediate glial scar formation and inhibition of axonal regeneration. Surface markers of common M1 macrophages include CD16/32, inducible nitric oxide synthase (iNOS), and CD86. Upon induction by IL-4, IL-10, transforming growth factor beta (TGF-β), and vascular endothelial growth factor (VEGF), macrophages can differentiate into M2 macrophages, which have a strong phagocytic effect and can devour and remove necrotic cells and degenerative tissues. M2 macrophages can also secrete anti-inflammatory factors (IL-4, IL-10, IL-13, and TGF-β) and nutrients (nerve growth factor and ciliary neurotrophic factor) that promote the degradation of glial scars, inhibit the inflammatory response, exert a neuroprotective effect, and accelerate the differentiation of nerve stem cells in the spinal cord into neurons. Surface markers of common M2 macrophages include CD206, arginase-1 (Arg-1), and CD209. In summary, the ratio of M1-type macrophages to M2 macrophages constitutes a determining factor for SCI outcome. Research shows that M1 macrophages are dominant during the early stage of SCI [7], although the function and phenotype of macrophages can change dynamically with the microenvironment of the SCI site [8,9]. Therefore, promoting the conversion of M1 type macrophages into M2 macrophages is crucial for promoting the repair of SCI.

It has been reported that several types of stem cells might induce the polarization of M1 macrophages into M2 macrophages including mesenchymal stem cells (MSCs) and nerve stem/precursor cells [9,10]. Abumaree et al. [11] demonstrated that MSCs play a role as immune suppressive cells by shifting macrophage differentiation from an inflammatory M1 to an anti-inflammatory M2 phenotype. Busch et al. [12] confirmed that MSCs can antagonize the axonal injury induced by macrophages during SCI and promote axonal regeneration by converting M1 type macrophages into M2 macrophages. In addition, after transplantation to the SCI site during the acute phase, MSCs can alter the state of macrophage activation, promoting the M1-to-M2 conversion of macrophages and thereby improving movement functions in SCI rats [12].

However, in recent years, the neural differentiation potential of MSCs has been controversial. For example, Hideaki et al. did not detect the conversion of MSCs into neurons or glial cells after transplantation into SCI model rats [13]. Typical adult MSCs, comprising bone marrow mesenchymal cells (BMSCs), should be isolated through ilium puncture. However, this process can cause secondary trauma to the patient; moreover, the stem cell content in adult bone marrow is very low (0.001–0.01%) [14], and the proliferation and differentiation ability of these cells decreases with age [15]. These defects limit the clinical application of BMSCs. Alternatively, neural stem cell transplantation can potentially result in neuronal/glial cell differentiation and can be coordinated with other cytokines to change the microenvironment of the injured spinal cord, making it more conducive to M2 macrophage polarization [16]. However, an ethical controversy exists regarding obtaining neural stem/precursor cells from aborted fetuses, although it is otherwise difficult to obtain adult nerve stem/precursor cells. Therefore, sources of stem cells that are noninvasive, age-independent, and can potentially promote SCI repair are urgently needed.

Hair dermal papillae are rich in pluripotent stem cells. They also comprise an advantageous source as they can be isolated by picking hair (without trauma), are available throughout the lifetime of the individual, and the number of stem cells is not limited by age. In addition, research shows that facial hair papillae constitute an enriched source of precursor cells that exhibit embryonic neural crest stem cell properties, along with the potential to differentiate into neurons/glial cells [17,18]. Previously, we found that a small proportion (1.14%) of neural crest stem cells carry the potential for neurodifferentiation [19]. In addition, the amount of brain-derived neurotrophic factor (BDNF) secreted by dermal papilla cells (DPCs) was significantly higher than that secreted by BMSCs [19]. Furthermore, injection of lenti-BDNF at the lesion site promoted M2 macrophage polarization and inhibited inflammatory responses after SCI in mice [20]; however, the exact mechanism through which this occurred has not been elucidated. After transplantation into rats subjected to spinal cord transection, and in the acute phase of SCI, DPCs can better antagonize the death of transplanted cells due to inflammation, compared to BMSCs. In addition, the number of DPCs in transected spinal cord-lesion sites was significantly higher than that of BMSCs [21]. These results suggest that DPCs have immunomodulatory characteristics that can inhibit the occurrence of an acute inflammatory response during SCI. Moreover, our data demonstrated that DPCs promote greater tissue repair after complete SCI than BMSCs, as evidenced by the enhanced number of axons formed within the lesion sites in the DPC-transplant group on day 21 post-transplantation [21]. Based on these findings, we hypothesized that DPCs play a role in promoting SCI repair by regulating the conversion of M1 macrophages to M2 macrophages, thus improving inflammation in the SCI microenvironment.

To test this hypothesis, the aim of this study was to further explore the mechanism through which DPCs promote SCI repair and to identify an ideal autologous stem cell source with immunomodulatory properties and neural differentiation potential. Accordingly, in this study we isolated bone marrow-derived macrophages (BMDMs) and induced them to differentiate into M1 macrophages to recapitulate the early stage of SCI (i.e., M1 prominence). We then investigated the regulatory effect of DPCs on the polarization of M1 macrophages into M2 macrophages through co-culture, and compared the effects of DPCs to those of BMSCs isolated from the same donor rat to assess their potential for cell transplantation therapy to treat acute-phase SCI.

2. Materials and methods

2.1. Animals

Adult Wistar rats (200–250 g, n = 6) were supplied by the Experimental Animal Center of Jilin University. All experimental procedures were approved by the ethics committee of Jilin University and conformed to the regulatory standards.

2.2. Isolation and cultivation of DPCs and BMSCs

DPCs were isolated and cultured as described [19]. Half of the medium was changed every 3 days. When the DPCs reached ~80% confluence, the medium was removed, the cells were rinsed twice with phosphate-buffered saline (PBS), and digested with 0.25% trypsin (Invitrogen, Carlsbad, CA) and 0.02% EDTA (Sigma, St. Louis, USA). When most DPCs had detached, an equal volume of Dulbecco's modified Eagle's medium (DMEM)/F-12 culture medium (Gibco, Paisley, UK)

containing 10% (*v*/v) fetal bovine serum (FBS; HyClone, Logan, UT) was added to terminate the digestion. The liquid was transferred to a centrifuge tube, centrifuged at 402 ×*g* for 5 min, and cell pellets were collected and resuspended in fresh proliferation medium consisting of DMEM/F-12 (1:1) medium supplemented with 10% (v/v) FBS and 10 ng/ml basic fibroblast growth factor (PeproTech, London, UK). Subsequently, the cells were expanded in new culture dishes at 1×10^4 cells/cm^2. Finally, DPCs at passage 4–7 were prepared for follow-up experiments. As a control, BMSCs were isolated from the same donor rat and cultured as described [19].

2.3. Isolation and cultivation of BMDMs from rats

For BMDM isolation, rats were deeply anesthetized via intraperitoneal injection of pentobarbital sodium (30 mg per kilogram of body weight) and sacrificed by cervical dislocation. The limbs of Wistar rats were dissected and maintained in PBS containing 5% (*v*/v) penicillin and streptomycin (HyClone) under sterile conditions. After removal of the musculature and connective tissue, the femur and tibia were rinsed with PBS, and their epiphyses were carefully cut with a bone cutter. The bone marrow was flushed using a 5-ml syringe containing PBS and centrifuged for 5 min at 402 ×*g* at room temperature. The pellets were suspended in PBS, filtered through 40-μm filters, and then re-centrifuged at 402 ×*g* for 5 min. Next, each pellet was suspended in high-glucose DMEM (Gibco) supplemented with 20% (*v*/v) FBS, 1% (v/v) penicillin and streptomycin, and 40 ng/ml GM-CSF (PeproTech) (hereafter referred to as BMDM-proliferation medium) for further culture. Half of the medium was changed every 3 days.

2.4. Validation of the M1-macrophage polarization model

Primary BMDMs were cultured in BMDM-proliferation medium for 7 days, and then cultured for 3 days in high-glucose DMEM supplemented with 20% (*v*/v) FBS, 1% (v/v) penicillin and streptomycin, 40 ng/ml GM-CSF, 100 ng/ml LPS (Sigma), and 20 ng/ml IFN-γ (PeproTech) (hereafter referred to as M1-macrophage induction medium).

2.5. DPC/BMSC co-culture with M1 macrophages

Primary BMDMs seeded in 6-well plates were cultured in BMDM-proliferation medium for 7 days, and then in M1-macrophage induction medium for 3 days. For co-culture experiments, DPCs or BMSCs at passage 6 were seeded with macrophages in transwell chambers (0.4-μm orifice) at a 1:1, 1:5, or 1:10 ratio, and cultured in M1-macrophage induction medium for 6, 12, or 24 h. For the control group (CG), an equivalent volume of M1-macrophage induction medium was added to the chamber, without cells.

2.6. Reverse-transcription-polymerase chain reaction (RT-PCR)

Total RNA from cells was extracted using the Trizol reagent (Invitrogen). cDNA was synthesized from 500 ng of total RNA with the Takara RNA PCR Kit (AMV) Version 3.0 (Takara, Dalian, China), using only the reagents for the reverse transcription protocol. The reaction conditions were as follows: 45 °C for 30 min, 99 °C for 5 min, and 5 °C for 5 min. PCR was performed with 1 μL of cDNA in a 20-μL reaction volume using 2× Taq Master Mix (Kang Wei Shi Ji, Beijing, China). A negative control reaction was performed using H_2O as the template. The reaction conditions were as follows: initial denaturation at 94 °C for 2 min; 30 cycles of denaturation at 94 °C for 30 s, annealing at 60–65 °C for 30 s, and extension at 72 °C for 50 s; and a final extension at 72 °C for 10 min. PCR products were separated by 1.5% agarose gel electrophoresis with ethidium bromide and visualized using an ultraviolet transilluminator. Primers were synthesized by Shanghai Sheng Gong Biological Engineering Co., LTD. The sequences of the primers used are shown in Table 1.

Table 1
Sequences and annealing temperatures of primers used for PCR.

Gene	Primer sequence (5′ to 3′)	Annealing temperature
ALP	TCCATGGTGGATTATGCTCA TTCTGTTCCTGCTCGAGGTT	60 °C
Sox2	GCACATGAACGGCTGGAGCAACG TGCTGCGAGTAGGACATGCTGTAGG	65 °C

2.7. Real-time quantitative-PCR (real-time qPCR)

Total RNA was reverse transcribed into cDNA using the Takara RNA PCR Kit (AMV), version 3.0 (Takara, Dalian, China). Only the reagents for the reverse transcription protocol were used. Real-time qPCR was performed using TransScript® Green Two-Step qRT-PCR SuperMix (TransGen Biotech, Beijing, China). GAPDH was used as an internal normalized reference for mRNA expression. PCR was performed in a PCR System 7300 (Applied Biosystems, Carlsbad, USA). The thermocycling conditions were as follows: 50 °C for 2 min; 95 °C for 10 min; and 40 cycles of 95 °C for 15 s and 60 °C for 1 min, 95 °C for 15 s, 60 °C for 1 min, and 95 °C for 15 s. mRNAs expression was measured using cycle threshold (CT) values, and the results were converted to fold-changes [22]. The sequences of the primers used are shown in Table 2.

2.8. Alkaline phosphatase (ALP) staining

Primary DPCs were fixed with 4% paraformaldehyde (Tripod, Beijing, China) at room temperature for 10 min, and ALP expression was detected using a BCIP/NBT ALP Color Development Kit (Bi Yuntian, Shanghai, China).

2.9. Flow cytometry analysis

Cells were trypsinized and counted. Approximately 1×10^6 cells were used for each test; cells were rinsed with 0.01 M PBS by centrifugation, fixed in 4% paraformaldehyde at room temperature for

Table 2
Sequences of primers used for real-time qPCR.

Gene	Primer sequence (5′ to 3′)
IL-1β	TCCATGGTGGATTATGCTCA TTCTGTTCCTGCTCGAGGTT
IL-4	CACCTCTCAAGCAGAGCACAG GGGTTCCATGGTGAAGTCAAC
IL-6	CTGCCCTTCAGGAACAGCTATG GGCAGTGGCTGTCAACAACAT
IL-10	ACTGCTAGTTTGCCTGCTCTT ATGTGGGTCTGGCTGACTGG
TNF-α	GAGATGTGGAACTGGCAGAGGA TCAGTAGACAGAAGAGCGTGGTG
TGF-β1	CTCCCGTGGCTTCTAGTGC GCCTTAGTTTGGACAGGATCTG
VEGFA	CCTGGCTTTACTGCTGTACCT GCTGGTAGACGTCCATGAACT
CD86	TCCTCCAGCAGTGGGAAACA TTTGTAGGTTTCGGGTATCCT
iNOS	CCTGGTGCAAGGGATCTTGG GAGGGCTTGCCTGAGTGAG
CD163	CTCAGCGTCTCTGCTGTCAC GGCCAGTCTCAGTTCCTTCT
CD206	AGTTGGGTTCTCCTGTAGCCCAA ACTACTACCTGAGCCCACACCTGCT
Arg-1	TGAACCCAACTCTTGGGAAG GTGATGCCCCAGATGACTTT
GAPDH	ATGGGAAGCTGGTCATCAAC GGATGCAGGGATGATGTTCT

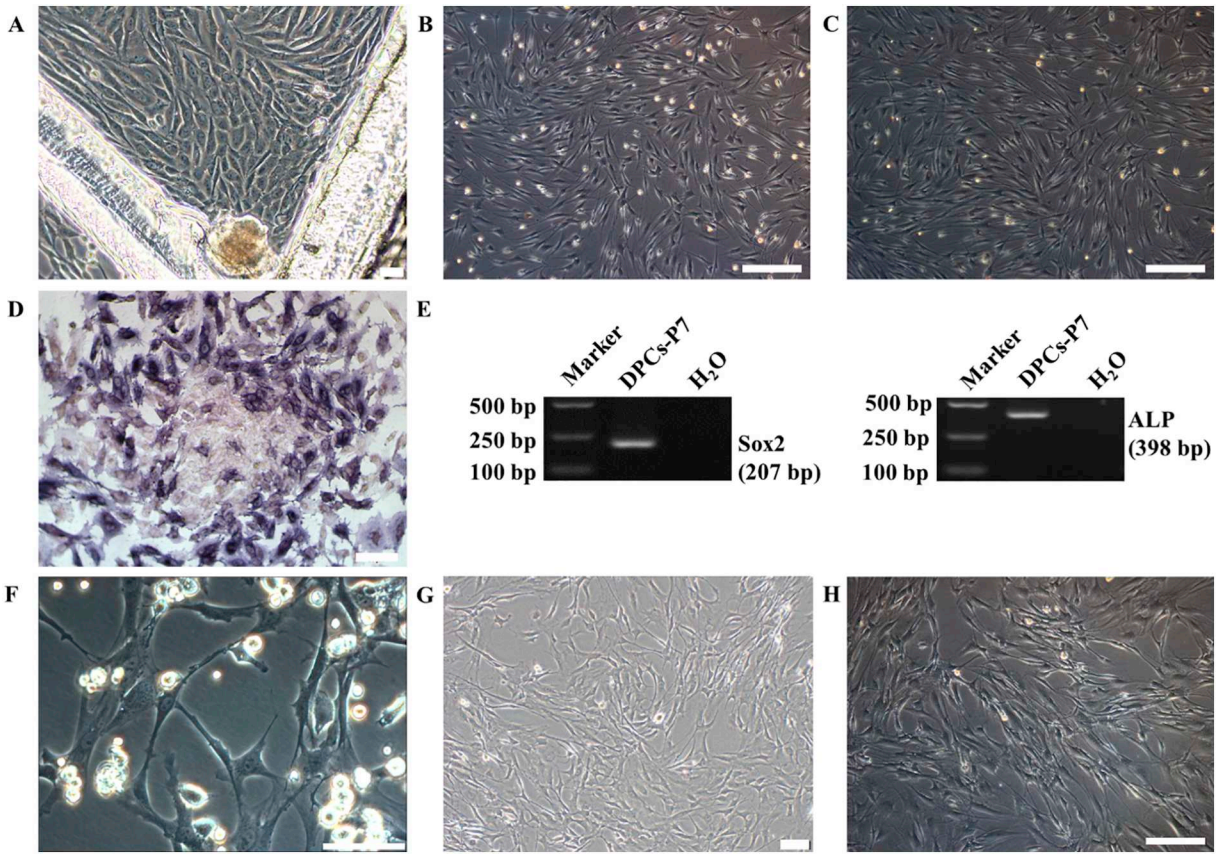

Fig. 1. Dermal papilla cells (DPCs) expressed dermal papilla-specific markers and had similar morphology with bone marrow mesenchymal stem cells (BMSCs). (A–E) Isolation, cultivation, and identification of DPCs. Spindle-shaped fibrocyte-like cells grew out from the "water-drop" shaped dermal papilla (A). Phase-contrast images showing the morphological characteristics of DPCs at passage 3 (B) or passage 7 (C). Most primary DPCs expressed alkaline phosphatase (ALP) (D). Reverse-transcription-polymerase chain reaction (RT-PCR) analysis confirmed the expression of dermal papillae markers ALP and Sox2 in DPCs. A negative control was established using H_2O as the template (E). (F–H) Isolation and cultivation of BMSCs. Phase-contrast images showing the morphological characteristics of primary BMSCs (F), BMSCs at passage 3 (G), and those at passage 7 (H). P: passage. Scale bars: (A) 20 μm, (B, C, H) 200 μm, (D, F, G) 50 μm.

10 min, and rinsed with PBS by centrifugation. Subsequently, 1% BSA/PBS (Biotopped, Beijing, China) was added to block non-specific binding. Next, the cells were incubated with primary antibodies for 1 h against CD31 (1:20; ab28364; Abcam, Cambridge, UK), CD44 (1:800; #5640; Cell Signaling Technology, Danvers, USA), CD45 (1:100; #05–1410; Millipore, Massachusetts, USA), CD90 (1:50; MAB1406; Millipore), CD105 (1:100; #05–1424; Millipore), CD68 (1:100; ab31630; Abcam), iNOS (1:20; ab15323; Abcam), or CD206 (1:400; ab64693; Abcam). The cells were then incubated with Alexa Fluor 488/555-conjugated secondary antibodies (1:1000; Cell Signaling Technology) for 1 h. Nuclei were stained with Hoechst 33342, and labeled cells were thoroughly washed with PBS and analyzed using on a FACSCalibur flow cytometer (BD Biosciences, San Jose, CA). Primary antibodies were omitted as a negative control.

2.10. Multipotent differentiation assay

The multipotency of DPCs was evaluated by inducing the cells to differentiate into mesodermal cell types (adipogenic and osteogenic) under the culture conditions described below.

Adipogenic differentiation was induced by culturing cells at 90% confluence in DMEM/F-12 (1:1) medium supplemented with 10% (*v*/v) FBS, 0.5 mM IBMX (Sigma), 0.2 mM Indocin (Sigma), 1 μM dexamethasone (Sigma), and 10 mg/L insulin (Sigma) for 2 weeks. Half of the medium was changed every 3 days. Intracellular lipid droplets were detected by Oil-Red O staining [23].

Osteogenic differentiation was induced by culturing cells at 90% confluence in DMEM/F-12 (1:1) medium supplemented with 10% (v/v) FBS, 0.1 μM dexamethasone, 50 μg/ml L-ascorbic acid 2-phosphate (Sigma), and 10 mM β-glycerophosphate (Sigma) for 2 weeks. Half of the medium was changed every 3 days. Mineralized bone nodules were detected by Alizarin Red-S staining [23].

2.11. α-Naphthyl acetate esterase (ANAE) staining

ANAE expression was detected using an ANAE Staining Kit (Ha Ling Sheng Wu, Shanghai, China). For quantification, images from 10 fields/well were randomly selected under a microscope at 100× magnification, and the positive expression rate was expressed as the ratio of ANAE-positive cells to the total number of cells.

2.12. Immunofluorescent cytochemical staining

Cells were fixed in 4% paraformaldehyde for 10 min. Subsequently, 1% BSA was used to block non-specific binding. Cells were then incubated with a primary antibody against CD68 (1:100; ab31630; Abcam) at 4 °C overnight. Samples were then incubated with Alexa Fluor 488-conjugated anti-mouse secondary antibodies (1:400, Cell Signal) for 1 h at room temperature. Nuclei were stained with Hoechst 33342.

2.13. Western blotting

Proteins were fractionated by sodium dodecyl sulfate-polyacrylamide gel electrophoresis and electrotransferred to a polyvinylidene difluoride membrane. Blots were first incubated for 1 h in

blocking buffer (0.1% Tween-20 [Sigma] and 5% nonfat powdered milk) at room temperature and then overnight at 4 °C with a primary antibody. Primary antibodies against the following proteins were used: CD68 (1:500; ab31630; Abcam), iNOS (1:40; ab15323; Abcam), CD206 (1:500; ab64693; Abcam), TNF-α (1:2000; 60,291–1-Ig; Proteintech, Chicago, USA), IL-10 (1:500; ab9969; Abcam), and VEGFA (1:800; 19,003–1-AP; Proteintech). A horseradish peroxidase-conjugated goat anti-mouse/rabbit secondary antibody (1:2000; Zhongshanjinqiao, Beijing, China) was then used, and antigen–antibody complexes were detected by chemiluminescence using the BeyoECL Plus Kit (Bi Yuntian).

2.14. Statistical analysis

Statistical analysis was performed using SPSS software version 11.0. Data are presented as the mean ± standard error of the mean from ≥3 independent experiments. Multiple group comparisons were made by performing one-way analysis of variance, followed by least-significant difference post-hoc comparisons (equal variances assumed) or Dunn's post-hoc test (unequal variances) for multiple comparisons. Differences between groups were considered statistically significant at $P < 0.05$.

3. Results

3.1. DPCs expressed dermal papilla-specific markers and had similar morphology compared with BMSCs

After 2 days of cultivation, typical spindle-shaped, fibrocyte-like cells grew from the papilla-like structure (Fig. 1A). After three passages, the cells still showed prominent proliferative activity, and approximately 5 days later, they self-arranged in a swirl that formed a confluent monolayer (Fig. 1B). After seven passages, the cells still displayed good growth and fibrocyte-like morphology (Fig. 1C). To investigate whether these cells expressed the DPC-specific markers, we performed ALP staining and RT-PCR. Most outward-migrating cells expressed ALP, and positive reactions were identified by the formation of blue-violet precipitates (Fig. 1D). RT-PCR results also revealed the expression of ALP and Sox2 in DPCs at passage 7 (Fig. 1E). These results indicated that we successfully isolated and cultured DPCs from rat vibrissa follicles.

We simultaneously harvested bone marrow from the same donor rat and cultured primary BMSCs. After 1 week of culture, spindle-shaped adherent cells were observed (Fig. 1F). After three passages, the cells still showed a typical fibroblast-like morphology and were arranged in a swirl pattern (Fig. 1G). The proliferation rate declined with passage; after seven passages, cell proliferation rate had obviously decreased, and the cells had adopted a flattened and spread out morphology (Fig. 1H).

The cell morphology and arrangement of DPCs were similar to those of BMSCs; therefore, DPCs might have some characteristics of BMSCs.

3.2. DPCs had an MSC phenotype and were capable of multipotent differentiation

Flow cytometry analysis revealed high positive-expression rates for CD44 (98.27%), CD90 (99.82%), and CD105 (94.48%), and low positive-expression rates for CD31 (6.8%) and CD45 (0.38%) in DPCs (Fig. 2A). Because the expression patterns of MSC markers were similar to those of BMSCs (Fig. 2B), we speculated that DPCs might be capable of multipotent differentiation and immunoregulation (as observed for BMSCs).

After induction for 2 weeks, intracellular lipid droplets formed. Adipogenesis was evaluated by Oil Red O staining. Lipid droplets in DPCs were smaller and less obvious (Fig. 2C) than those of BMSCs (Fig. 2D).

After induction for 2 weeks, calcium nodules were formed. Osteogenesis was evaluated by Alizarin red staining. The calcium nodules outside DPCs were not massively formed (Fig. 2E), as compared with those outside BMSCs (Fig. 2F).

These results indicate that DPCs differentiated into adipocytes and osteoblasts under specific conditions, but that the differentiation capacity of the mesenchymal lineages was impaired for DPCs, compared with BMSCs.

3.3. BMDMs were induced into M1 macrophages in vitro

After 7 days of primary cultivation, cells exhibited a flattened morphology. Some cells had round, oval, or long spindle shapes, whereas one or more pseudo feet extended from other cells (Fig. 3A). The expression of ANAE, a known, typical macrophage marker, was revealed by ANAE staining, and a positive reaction was identified by the precipitation of brown-, red-, or violet-colored precipitates (Fig. 3B). The proportion of positive cells was 93.64% ± 11.15% for BMDMs. Immunofluorescent staining and western blotting showed that BMDMs were positive for the macrophage-specific marker CD68 (Fig. 3C and D). Flow cytometry analysis further revealed the high expression rate of CD68 (91.01%; Fig. 3E) and the low expression rate of the M1-specific marker iNOS (0.62%; Fig. 3F) and the M2-specific protein CD206 (1.3%; Fig. 3G). Thus, we deduced that the primary cultured cells were un-activated macrophages (M0).

At the beginning of induction, BMDMs were round or oval, and long processus pseudopodia protruded from some cells (Fig. 3H). After 3 days of induction, most cells became round, resembling “fried eggs.” The morphology of these cells was typical of M1 macrophages (Fig. 3I). To investigate whether these cells expressed an M1-macrophage marker, we performed flow cytometry. The cells were positive for the macrophage marker CD68, with a positive expression ratio of 89.53% (Fig. 3J), as well as the M1-macrophage marker iNOS, with a positive expression ratio of 84.1% (Fig. 3K). Most cells were negative for the M2-macrophage marker CD206 (0.42% positive; Fig. 3L). These results indicated that we had successfully induced BMDMs to differentiate into M1-macrophages in vitro.

3.4. Co-culturing with DPCs induced the conversion of M1-type macrophages into M2-type macrophages

3.4.1. Cell proportion and timing of co-culture

To investigate the appropriate cell proportion and duration for co-culture, we examined trends in the expression of characteristic cytokines and specific markers of M1 and M2 macrophages under different conditions by qRT-PCR. This analysis revealed relatively low expression of M1 macrophage-characteristic cytokines (IL-1β, IL-6, and TNF-α) when DPCs or BMSCs were co-cultured with macrophages at a 1:1 ratio for 24 h (Fig. 4A and B). This was also true for the M1 macrophage-specific markers CD86 and iNOS (Fig. 4A and B). Meanwhile, the expression level of cytokines characteristic of M2 macrophages (IL-4, IL-10, TGF-β, and VEGFA) was highest (Fig. 4C and D), which was also true for the M2 macrophage-specific markers CD163, CD206, and Arg-1 (Fig. 4C and D). Thus, we performed 24-h cell cultivations with a 1:1 ratio in subsequent experiments.

3.4.2. DPCs converted macrophages to the M2 phenotype upon co-culture

After 0 h of co-culture at a 1:1 ratio, cells in the lower chamber resembled “fried eggs,” which was the typical morphology of the M1 macrophages in the DPC group (Fig. 5A). After co-culture for 24 h, the cells became elongated and spindle-like, which was the typical morphology of M2 macrophages (Fig. 5B). The same phenomenon was also observed in the BMSC group after co-culture for 0 h (Fig. 5C) or 24 h (Fig. 5D). However, in the CG, cells in the lower chamber retained their fried egg-like morphology after culturing for either 0 (Fig. 5E) or 24 h (Fig. 5F).

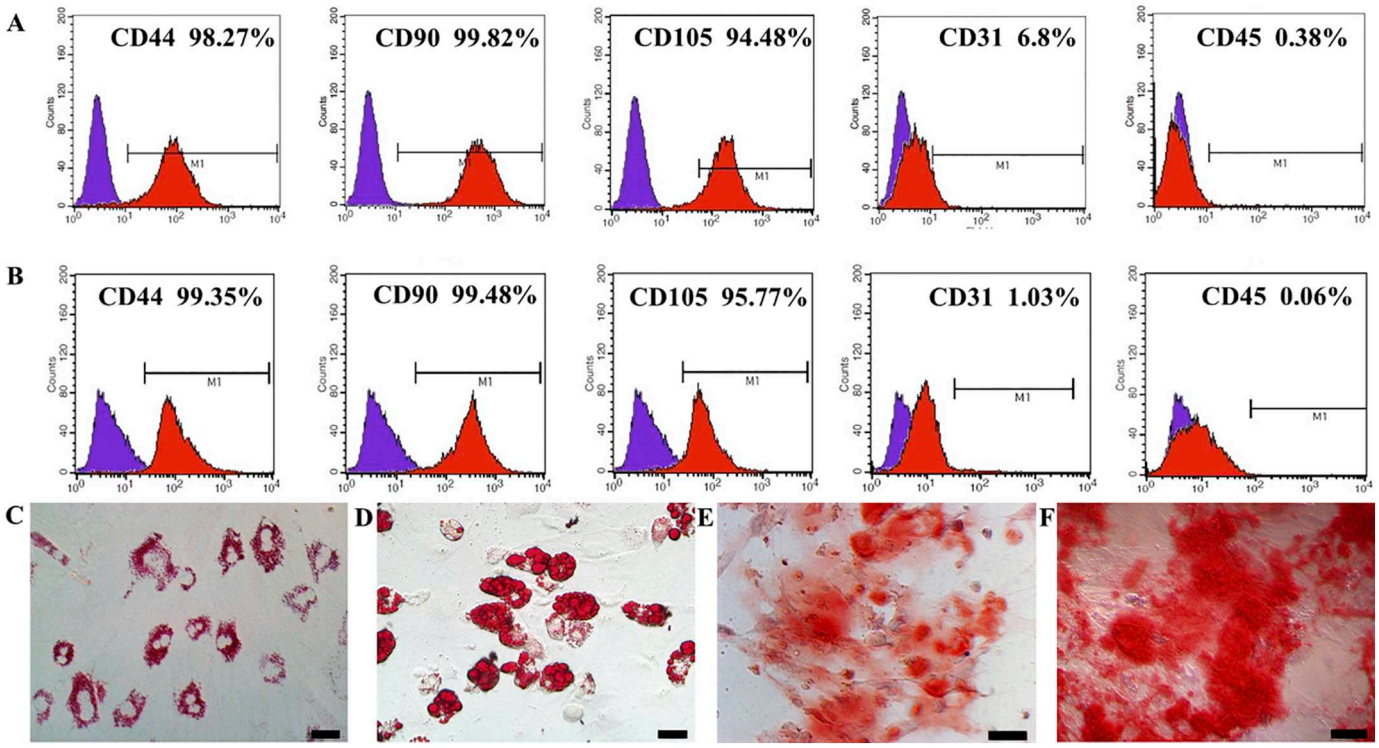

Fig. 2. DPCs had a mesenchymal stem cell phenotype and were capable of multipotent differentiation. (A, B) Flow cytometry revealed the expression of mesenchymal stem cell (MSC) markers in DPCs (A), which was similar to that in bone marrow mesenchymal stem cell (BMSCs) (B). (C–F) DPCs and BMSCs exhibited multipotent differentiation potential. Oil Red O staining showed the formation of intracellular lipid droplets in DPCs (C) and BMSCs (D) after induction for 2 weeks. Alizarin red staining showed the formation of calcium nodules outside DPCs (E) and BMSCs (F) after induction for 2 weeks. Scale bars: (C and D) 20 μm, (E and F) 50 μm.

3.4.3. DPCs induced downregulation of M1 macrophage-characteristic cytokines and upregulation of M2 macrophage-characteristic cytokines, as well as specific markers

To investigate changes in the expression of cytokines characteristic of M1/M2-macrophages after co-culture, we performed qRT-PCR and western blotting. qRT-PCR analysis revealed that, compared to the levels in the BMSC and CGs, the DPC group exhibited lower levels of the M1 macrophage-characteristic cytokines TNF-α (DPC group versus BMSC group, $P = .00159$; DPC group versus CG, $P = .00143$) and IL-6 (DPC group versus BMSC group, $P = .00319$; DPC group versus CG, $P = .05709$) and higher levels of the M2 macrophage-characteristic cytokines IL-10 (DPC group versus BMSC group, $P = .03434$; DPC group versus CG, $P = .00151$) and VEGFA (P = .00159). In contrast, the expression levels of IL-1β, IL-4, and TGF-β were similar to those in the BMSC group ($P = .92297$, 0.69906, 0.92127, respectively) and the CG ($P = .06605$, 0.19728, 0.15920, respectively) (Fig. 6A). Moreover, we detected TNF-α, IL-10, and VEGFA expression in the DPC and BMSC groups, as well as the CG, by western blot analysis. TNF-α expression was lower in the DPC group than in the BMSC group ($P = .04795$) and CG ($P = .00221$); IL-10 expression in the DPC group was similar to that in the BMSC group ($P = .95116$), but was higher than that in the CG ($P = .02770$); VEGFA expression was similar to that in the BMSC group ($P = .61183$) and CG ($P = .33367$; Fig. 6B).

To investigate changes in M1/M2-macrophage-specific marker expression after co-culturing, we performed qRT-PCR and western blotting. qRT-PCR analysis revealed that the expression level of the M1-macrophage-specific marker iNOS in the DPC group was similar to that in the BMSC group ($P = .21360$), but was lower than that in the CG ($P = .00674$). In addition, CD86 expression in the DPC group was lower than that in the BMSC group ($P = .00244$) and CG ($P = .00002$). CD163 expression in the DPC group was similar to that in the BMSC group ($P = .83444$) and CG ($P = .11133$). Expression of the M2-macrophage-specific marker CD206 in the DPC group was similar to that in the BMSC group ($P = .41440$), but was higher than that in the CG ($P = .00029$); further, Arg1 expression in the DPC group was similar to that in the BMSC group ($P = .51380$) and CG ($P = .47271$; Fig. 6C).

Moreover, we detected iNOS and CD206 expression in the DPC group, BMSC group, and CG by western blot analysis. The results revealed that iNOS expression in the DPC group was similar to that in the BMSC group ($P = .11619$) and CG ($P = .10009$); CD206 expression in the DPC group was similar to that in the BMSC group ($P = .07047$), but was higher than that in CG ($P = .01918$; Fig. 6D).

3.4.4. DPCs decreased the proportion of M1 macrophages and increased the proportion of M2 macrophages

Flow cytometry analysis revealed that after co-culture with DPCs for 24 h, the proportion of $iNOS^+$ cells changed from 95.45% ± 2.41% to 54.06% ± 3.19%, and that of $CD206^+$ cells changed from 0.25% ± 0.24% to 43.39% ± 7.03. In contrast, after co-culture with BMSCs for 24 h, the proportion of $iNOS^+$ cells changed from 95.45% ± 2.41% to 61.42 ± 3.65%, and that of $CD206^+$ cells changed from 0.25% ± 0.24% to 38.1 ± 6.63% (Fig. 7A). In the DPC group, the proportion of $iNOS^+$ cells was significantly lower than that in the BMSC group ($P = .01654$) and the CG ($P = .00006$). However, the proportion of $CD206^+$ cells was similar to that in the BMSC group ($P = .39714$), but was significantly higher than that in the CG ($P = .00045$; Fig. 7B).

4. Discussion

BMSCs have therapeutic potential for tissue repair because of their capacity for multipotent differentiation and their ability to modulate immune responses; however, the clinical applications of BMSCs have limitations. Thus, there is a need to find other promising autologous

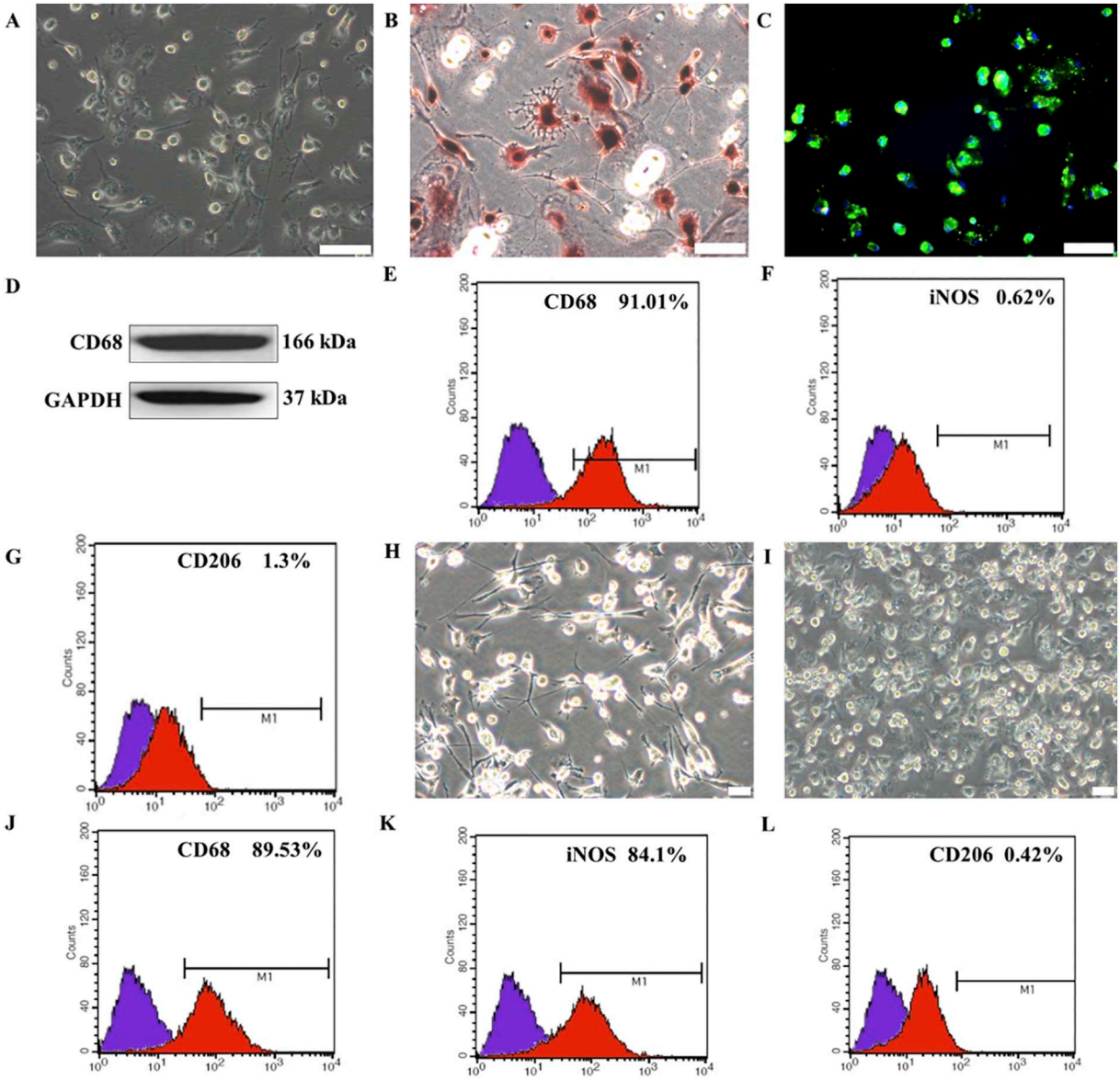

Fig. 3. Bone marrow-derived macrophages (BMDMs) were induced into M1 macrophages *in vitro*. (A–G) Isolation, cultivation, and identification of BMDMs. Phase-contrast images showing the morphological characteristics of primary BMDMs (A). BMDMs expressed α-naphthyl acetate esterase (ANAE) (B). Immunohistochemical staining and western blotting revealed the expression of CD68 in BMDMs (C, D). Flow cytometry further demonstrated a high positive expression rate of CD68, as well as a low positive expression rate of iNOS and CD206 (E–G). (H–L) Induction of BMDMs into M1-type macrophages. Before induction, the BMDMs were round or oval, and long processus pseudopodia protruded from some cells (H). After induction for 3 days, most cells became round, resembling "fried eggs." The morphology of the cells was typical of M1 macrophages (I). Flow cytometry further demonstrated the high positive expression rates of CD68 (J) and iNOS (K), as well as the low positive expression rate of CD206 (L). Scale bars: (A–C) 50 μm, (H and I) 20 μm.

sources of adult stem cells.

The dermal papilla, which is located at the base of the hair bulb, plays a leading role in regulating hair follicle development and periodical growth, and is also considered to be a rich source of pluripotent stem cells [24]. The papilla is composed of specialized mesenchymal cells, namely DPCs, which express specific enzymes and molecular markers. ALP is one of the markers used to identify DPCs and is also considered to be an indicator of hair-induced characteristics [25,26]. In addition, Sox2, known as an SRY-related transcription factor that promotes somatic stemness, has also been confirmed to be expressed in dermal papillae [27]. Similar to another report [28], we observed that monolayer-expanded DPCs strongly expressed the papillae markers ALP and Sox2, as well as MSC markers, with an expression pattern similar to that observed in BMSCs. In addition, DPCs were shown to have the capacity to differentiate into adipocytes and osteoblasts. However, we found that DPCs exhibited a weaker capacity for differentiating into mesenchymal lineages. Since craniofacial hair follicle papilla cells originate from the neural crest and reside in the craniofacial skin, DPCs are a primary source of skin-derived precursors, which have neural crest stem cell-like properties [18]. Thus, we speculate that DPCs tend to differentiate into neurons and glial cells under certain physiological and experimental conditions.

Previously, BMSCs were used in clinical trials for treating SCI, and according to the report the underlying mechanisms of functional recovery following BMSC transplantation are likely mediated by their abilities to secrete various soluble factors with trophic, proangiogenic, and anti-inflammatory functions [29]. However, to our knowledge, no reports have described the anti-inflammatory properties of DPCs. Previously, we observed that compared to those in BMSCs, DPCs showed higher expression levels of the angiogenesis factor VEGFA and anti-

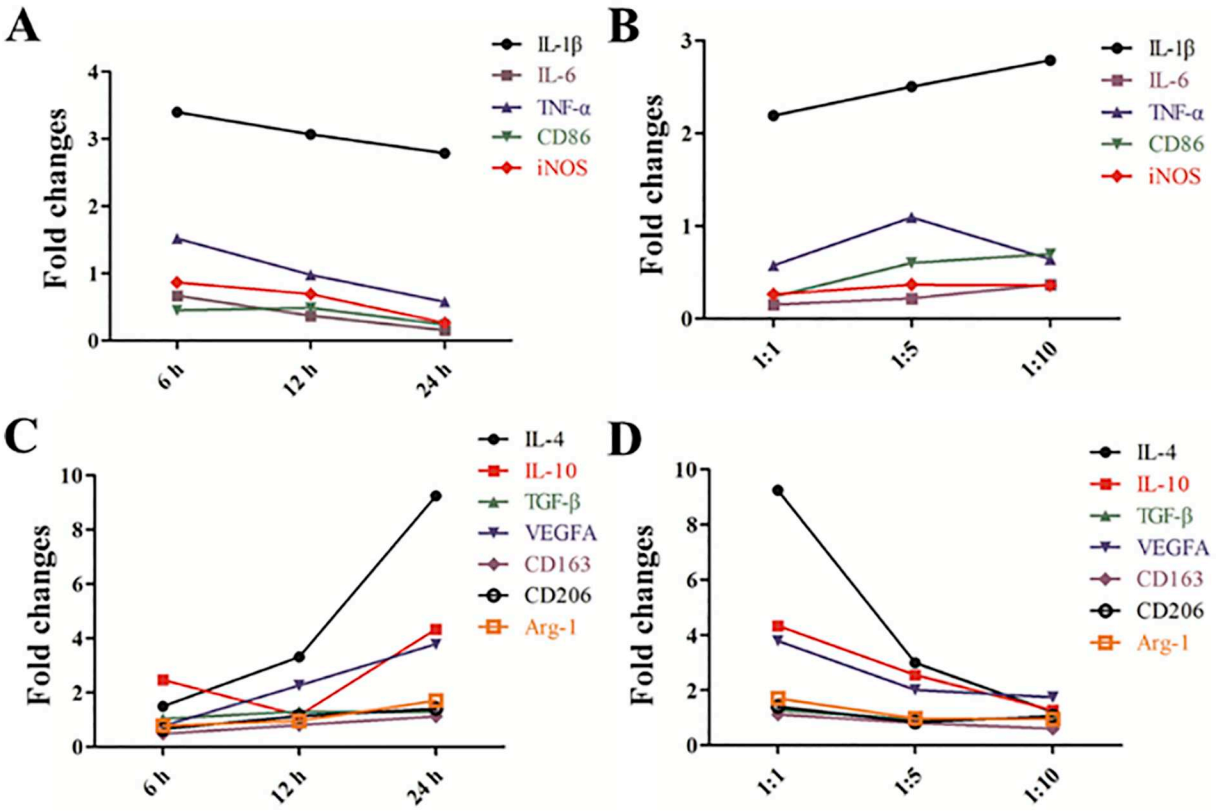

Fig. 4. Trends in the expression of characteristic cytokines and specific markers of M1/M2-macrophages with different cell proportions and durations of co-culture. (A) Relative expression levels of M1 macrophage-characteristic cytokines (IL-1β, IL-6, and TNF-α) and M1 macrophage-specific markers (CD86 and iNOS) after co-culture with dermal papilla cells for 6, 12, and 24 h, at a 1:1 ratio. (B) Relative mRNA-expression levels of M1 macrophage-characteristic cytokines IL-1β, IL-6, or TNF-α after co-culture with DPCs for 24 h at a 1:1, 1:5, or 1:10 ratio, respectively, as well as the M1 macrophage-specific markers CD86 and iNOS. (C) Relative expression levels of M2 macrophage-characteristic cytokines IL-4, IL-10, TGF-β, and VEGFA after co-culture with DPCs for 6 h, 12 h, or 24 h at a 1:1 ratio, as well as the M2 macrophage-specific markers CD163, CD206, and Arg-1. (D) Relative expression levels of M2 macrophage-characteristic cytokines IL-4, IL-10, TGF-β, and VEGFA after co-culture with DPCs for 24 h at a 1:1, 1:5, or 1:10 ratio, as well as the M2 macrophage-specific markers CD163, CD206, and Arg-1.

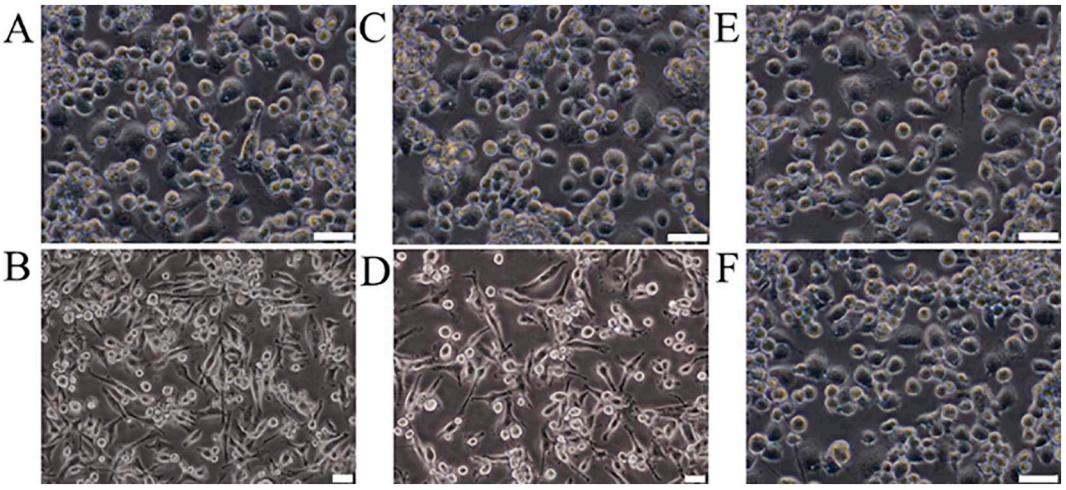

Fig. 5. DPCs converted macrophages to the M2 phenotype under transwell conditions. (A) After co-culture with DPCs for 0 h at a 1:1 ratio, cells in the lower chamber resembled "fried eggs," which is a typical morphology of M1 macrophages. (B) After co-culture with DPCs for 24 h, the cells acquired an elongated, spindle-like morphology, which is typical of M2 macrophages. (C, D) The same morphologic change in cells in the lower chamber was also observed after co-culture with BMSCs for 0 h (C) or 24 h (D). (E, F) In the control group, cells in the lower chamber remained "fried egg-like" after culturing for either 0 (E) or 24 h (F). Scale bars, 20 μm.

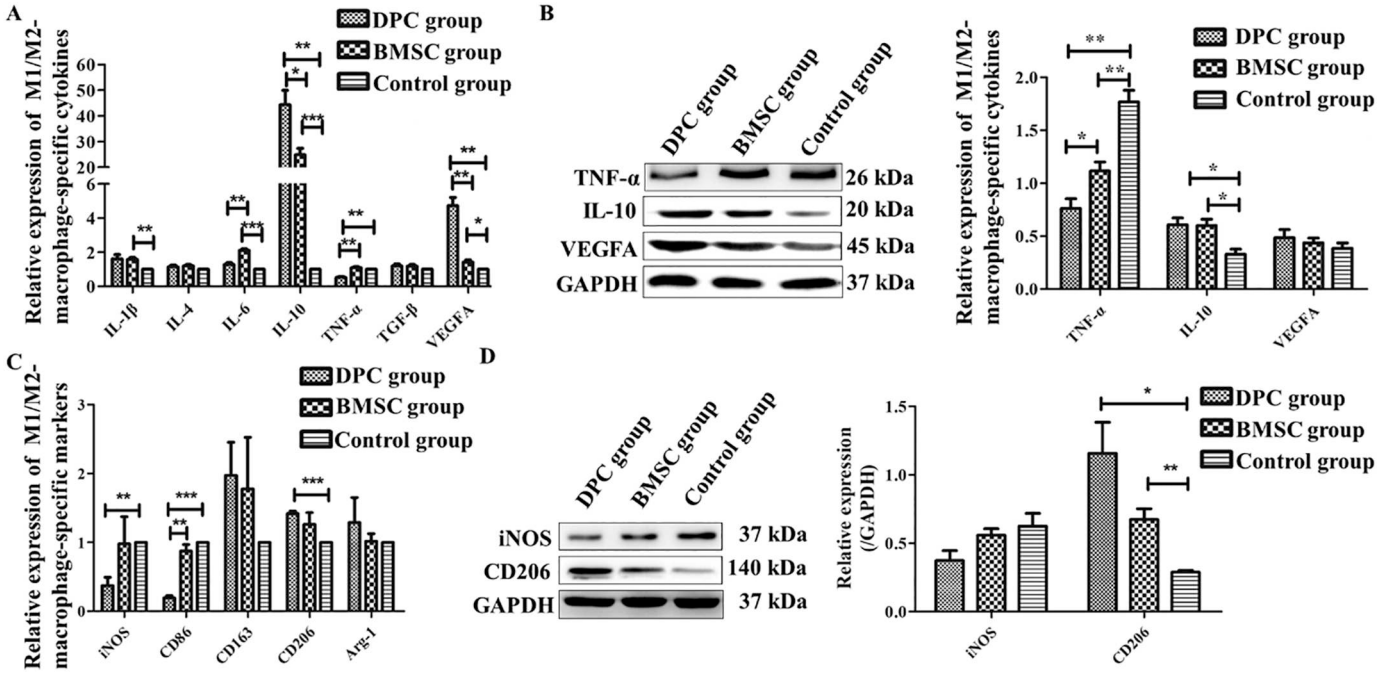

Fig. 6. DPCs induced downregulation of M1 macrophage-characteristic cytokines and upregulation of M2 macrophage-characteristic cytokines, as well as specific markers. (A) RT-qPCR analysis revealed that compared to those in BMSC and control groups, the DPC group produced lower levels of the M1 macrophage-characteristic cytokines TNF-α and IL-6 and higher levels of the M2 macrophage-characteristic cytokines IL-10 and VEGFA. However, the expression levels of IL-1β, IL-4, and TGF-β were similar to those in the BMSC and control groups. (B) Western blot analysis revealed that TNF-α expression was lower in the DPC group than in the BMSC and control groups; IL-10 expression was similar in the DPC group to that in the BMSC group, but was higher than that in the control group; VEGFA expression was similar to that in the BMSC and control groups. (C) RT-qPCR analysis revealed that the expression of the M1-macrophage-specific marker iNOS in the DPC group was similar to that in the BMSC group, but lower than that in the control group; CD86 expression in the DPC group was lower than that in the BMSC and control groups. CD163 expression in the DPC group was similar to that in the BMSC and control group. Expression of the M2-macrophage-specific marker CD206 in the DPC group was similar to that in the BMSC group, but higher than that in the control group; Arg1 expression in the DPC group was similar to that in the BMSC and control groups. (D) Western blotting revealed that iNOS expression was similar to that in the BMSC and control groups, and CD206 expression was similar to that in the BMSC group, but higher than that in the control group. $^{*}P < .05$, $^{**}P < .01$, $^{***}P < .001$, $n = 3$.

inflammatory cytokines IL-4 and IL-10, similar expression levels of the anti-inflammatory TGF-β, and lower expression levels of the pro-inflammatory cytokines TNF-α, IL-6, and IL-1β. Since IL-10, TGF-β, and VEGF play important roles in regulating the polarization of pro-inflammatory M1-type macrophages into anti-inflammatory M2-type macrophages [30,31], we suspect that DPCs have anti-inflammatory properties that are associated with regulating the conversion of M1 to M2 macrophages.

The ratio of M1:M2 cells is a significant factor for the repair of SCI. Therefore, increasing the M2 cell population in the injured local microenvironment might represent a promising strategy for tissue repair after SCI [32]. To our knowledge, this is the first in vitro study evaluating the effects of DPCs on the initial differentiation of macrophages using BMSCs as a positive control. This was accomplished by co-

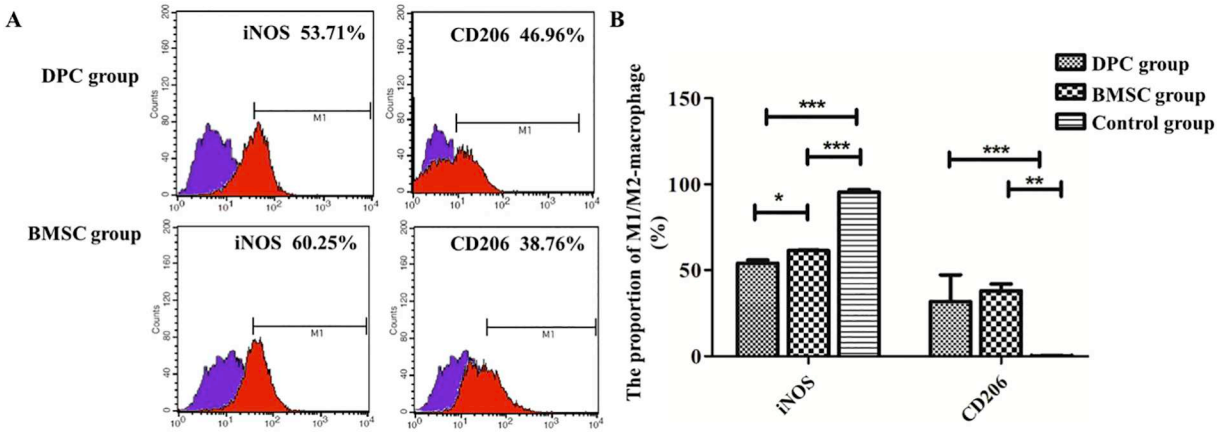

Fig. 7. DPCs decreased the proportion of M1 macrophages and increased the proportion of M2 macrophages. (A) Flow cytometry revealed that after co-culture with DPCs for 24 h, the proportion of $iNOS^{+}$ cells changed from 95.45% ± 2.41% to 54.06% ± 3.19%, and the ratio of $CD206^{+}$ cells changed from 0.25% ± 0.24% to 43.39% ± 7.03%. After co-culture with BMSCs for 24 h, the proportion of $iNOS^{+}$ cells changed from 95.45% ± 2.41% to 61.42% ± 3.65%, and the proportion of $CD206^{+}$ cells changed from 0.25% ± 0.24% to 38.10% ± 6.63%. (B) After co-culture for 24 h, the ratio of $iNOS^{+}$ cells in the DPC group was significantly lower than that in the BMSC and control groups. The ratio of $CD206^{+}$ cells was similar to that in the BMSC group, but was significantly higher than that in the control group. $^{*}P < .05$, $^{**}P < .01$, $^{***}P < .001$, n = 3.

culturing DPCs and BMSCs with macrophages, which were derived from normal rat peripheral blood monocytes grown in medium containing GM-CSF, LPS, and IFN-γ, which are inducers of M1 macrophage differentiation. After 3 days of culture, monocytes in GM-CSF medium differentiated into “fried egg-shaped” cells typical of M1-like macrophages. These M1-like macrophages expressed the macrophage marker CD68 and the M1 macrophage marker iNOS, but lacked expression of the characteristic M2 macrophage marker CD206. After adding DPCs or BMSCs to the initial culture of monocytes in the M1-macrophage induction medium, monocytes differentiated into elongated, spindle-like cells, which is a distinctive feature of M2-like macrophages. We also observed that expression of the cell-surface marker CD206 by M2-like macrophages significantly increased compared to that under control conditions. In addition, a dynamic increase in the number of M2 macrophages, characterized by increased expression of CD206, was observed. This finding further confirmed the classification of M2 macrophages, thus further supporting the notion that differentiation of monocytes into M2-like macrophages occurs in the presence of DPCs. These results demonstrated that DPCs can shift the initial differentiation of monocytes from M1 to M2 macrophages.

The M1 to M2 polarization of macrophages is a tightly controlled process involving a set of signaling pathways and transcriptional regulatory networks. BDNF, which is mainly expressed in the central nervous system, plays an important role in the development and differentiation of neurons [33]. Moreover, some evidence indicates that BDNF might be involved in regulating the immune response [34]. Previously, we observed that monolayer-expanded DPCs release greater quantities of BDNF into the extracellular environment than BMSCs [20]. Ji et al. [19] also demonstrated that local injection of lenti-BDNF at the lesion site promotes a shift from the M1 to the M2 phenotype and ameliorates the inflammatory microenvironment; this partially contributed to the functional recovery of locomotor activity after SCI, but the exact mechanism was unclear. It is well established that the effects of BDNF on cells are mediated by binding to its high-affinity receptor tropomyosin-related kinase B (TrkB), which drives activation of several intracellular signal transduction pathways, including PI3K/AKT, which in turn plays an important role in modulating the activation phenotype of macrophages. AKT comprises a family of three serine-threonine kinases (Akt1, Akt2, and Akt3). Akt1 and Akt2 differentially contribute to the polarization of macrophages, with Akt1 ablation giving rise to an M1 phenotype and Akt2 ablation resulting in an M2 phenotype [35,36]. As such, LY294002, an Akt inhibitor, enhances M1 marker expression [37]. Based on this observation, we speculate that DPCs modulate M1–M2 macrophage polarization via the TrkB/PI3K/AKT1-signaling pathway by secreting BDNF, although this possibility needs to be tested in further experiments.

In summary, our data demonstrate that DPCs from hair follicle dermal papilla have adult stem cell properties and the capacity to reprogram macrophages into an anti-inflammatory M2 phenotype in vitro. This might contribute to improvements in the adverse inflammatory microenvironment, thereby promoting tissue repair. These findings further support the notion that DPCs represent a unique population of MSCs with functional similarities to BMSCs. Specifically, their ease of isolation and tissue source accessibility indicate that they are a promising source for autologous cell therapy to treat SCI.

Declaration of interest

The authors declare that they have no conflict of interests regarding to the publication of this paper.

Acknowledgments

We thank Editage for their assistance with English editing during the preparation of this manuscript.

This work was supported by the Bethune program for Young Teachers from Jilin University [grant number 2015430] and the Outstanding Young Teacher's Training Program from Jilin University [grant number 419080500576]. Meiyig Li designed the study; analyzed the data; and wrote the manuscript. Meiyig Li and Yulin Li provided research funding.

References

[1] H.S. Chhabra, K. Sarda, Stem cell therapy in spinal trauma: does it have scientific validity? Indian. J. Orthop. 49 (2015) 56–71, https://doi.org/10.4103/0019-5413.143913.
[2] D. Tso, R.D. McKinnon, Cell replacement therapy for central nervous system diseases, Neural Regen. Res. 10 (2015) 1356–1358, https://doi.org/10.4103/1673-5374.165209.
[3] M. Nakamura, H. Okano, Cell transplantation therapies for spinal cord injury focusing on induced pluripotent stem cells, Cell Res. 23 (2013) 70–80, https://doi.org/10.1038/cr.2012.171.
[4] A.D. Greenhalgh, S. David, Differences in the phagocytic response of microglia and peripheral macrophages after spinal cord injury and its effects on cell death, J. Neurosci. 34 (2014) 6316–6322, https://doi.org/10.1523/JNEUROSCI.4912-13.2014.
[5] X. Zhou, X. He, Y. Ren, Function of microglia and macrophages in secondary damage after spinal cord injury, Neural Regen. Res. 9 (2014) 1787–1795, https://doi.org/10.4103/1673-5374.143423.
[6] J.R. Plemel, V. Wee Yong, D.P. Stirling, Immune modulatory therapies for spinal cord injury–past, present and future, Exp. Neurol. 258 (2014) 91–104, https://doi.org/10.1016/j.expneurol.2014.01.025.
[7] J.C. Gensel, B. Zhang, Macrophage activation and its role in repair and pathology after spinal cord injury, Brain Res. 1619 (2015) 1–11, https://doi.org/10.1016/j.brainres.2014.12.045.
[8] S. David, A.D. Greenhalgh, A. Kroner, Macrophage and microglial plasticity in the injured spinal cord, Neuroscience 307 (2015) 311–318, https://doi.org/10.1016/j.neuroscience.2015.08.064.
[9] Y. Ren, W. Young, Managing inflammation after spinal cord injury through manipulation of macrophage function, Neural Plast. 2013 (2013) 945034, https://doi.org/10.1155/2013/945034.
[10] G. Zheng, M. Ge, G. Qiu, Q. Shu, J. Xu, Mesenchymal stromal cells affect disease outcomes via macrophage polarization, Stem Cells Int. (2015) (2015) 989473, https://doi.org/10.1155/2015/989473.
[11] M.H. Abumaree, M.A. Al Jumah, B. Kalionis, D. Jawdat, A. Al Khaldi, F.M. Abomaray, A.S. Fatani, L.W. Chamley, B.A. Knawy, Human placental mesenchymal stem cells (pMSCs) play a role as immune suppressive cells by shifting macrophage differentiation from inflammatory M1 to anti-inflammatory M2 macrophages, Stem Cell Rev. 9 (2013) 620–641, https://doi.org/10.1007/s12015-013-9455-2.
[12] S.A. Busch, J.A. Hamilton, K.P. Horn, F.X. Cuascut, R. Cutrone, N. Lehman, R.J. Deans, A.E. Ting, R.W. Mays, J. Silver, Multipotent adult progenitor cells prevent macrophage-mediated axonal dieback and promote regrowth after spinal cord injury, J. Neurosci. 31 (2011) 944–953, https://doi.org/10.1523/JNEUROSCI.3566-10.2011.
[13] H. Nakajima, K. Uchida, A.R. Guerrero, S. Watanabe, D. Sugita, N. Takeura, A. Yoshida, G. Long, K.T. Wright, W.E. Johnson, H. Baba, Transplantation of mesenchymal stem cells promotes an alternative pathway of macrophage activation and functional recovery after spinal cord injury, J. Neurotrauma 29 (2012) 1614–1625, https://doi.org/10.1089/neu.2011.2109.
[14] M.F. Pittenger, A.M. MacKay, S.C. Beck, R.K. Jaiswal, R. Douglas, J.D. Mosca, M.A. Moorman, D.W. Simonetti, S. Craig, D.R. Marshak, Multilineage potential of adult human mesenchymal stem cells, Science 284 (1999) 143–147.
[15] O.S. Beane, V.C. Fonseca, L.L. Cooper, G. Koren, E.M. Darling, Impact of aging on the regenerative properties of bone marrow-, muscle-, and adipose-derived mesenchymal stem/stromal cells, PLoS One 9 (2014) e115963, , https://doi.org/10.1371/journal.pone.0115963.
[16] S. Nishimura, A. Yasuda, H. Iwai, M. Takano, Y. Kobayashi, S. Nori, O. Tsuji, K. Fujiyoshi, H. Ebise, Y. Toyama, H. Okano, M. Nakamura, Time-dependent changes in the microenvironment of injured spinal cord affects the therapeutic potential of neural stem cell transplantation for spinal cord injury, Mol. Brain 6 (2013) 3, https://doi.org/10.1186/1756-6606-6-3.
[17] D.P. Hunt, P.N. Morris, J. Sterling, J.A. Anderson, A. Joannides, C. Jahoda, A. Compston, S. Chandran, A highly enriched niche of precursor cells with neuronal and glial potential within the hair follicle dermal papilla of adult skin, Stem Cells 26 (2008) 163–172, https://doi.org/10.1634/stemcells.2007-0281.
[18] H. Jinno, O. Morozova, K.L. Jones, J.A. Biernaskie, M. Paris, R. Hosokawa, M.A. Rudnicki, Y. Chai, F. Rossi, M.A. Marra, F.D. Miller, Convergent genesis of an adult neural crest-like dermal stem cell from distinct developmental origins, Stem Cells 28 (2010) 2027–2040, https://doi.org/10.1002/stem.525.
[19] M. Li, J.Y. Liu, S. Wang, H. Xu, L. Cui, S. Lv, J. Xu, S. Liu, G. Chi, Y. Li, Multipotent neural crest stem cell-like cells from rat vibrissa dermal papilla induce neuronal differentiation of PC12 cells, Biomed. Res. Int. 2014 (2014) 186239, https://doi.org/10.1155/2014/186239.
[20] X.C. Ji, Y.Y. Dang, H.Y. Gao, Z.T. Wang, M. Gao, Y. Yang, H.T. Zhang, R.X. Xu, Local injection of Lenti-BDNF at the lesion site promotes M2 macrophage polarization and inhibits inflammatory response after spinal cord injury in mice, Cell. Mol. Neurobiol. 35 (2015) 881–890, https://doi.org/10.1007/s10571-015-0182-x.

[21] M.Y. Li, X.L. Mei, S. Lv, Z. Zhang, J. Xu, D. Sun, J. Xu, X. He, G. Chi, Y. Li, Rat vibrissa dermal papilla cells promote healing of spinal cord injury following transplantation, Exp. Ther. Med. 15 (2018) 3929–3939, https://doi.org/10.3892/etm.2018.5916.
[22] K.J. Livak, T.D. Schmittgen, Analysis of relative gene expression data using real-time quantitative PCR and the $2^{-\Delta\Delta C_T}$ method, Methods 25 (2001) 402–408, 2001, https://doi.org/10.1006/meth.2001.1262.
[23] T. Bai, F. Liu, F. Zou, G. Zhao, Y. Jiang, L. Liu, J. Shi, D. Hao, Q. Zhang, T. Zheng, Y. Zhang, M. Liu, S. Li, L. Qi, J.Y. Liu, Epidermal growth factor induces proliferation of hair follicle-derived mesenchymal stem cells through epidermal growth factor receptor-mediated activation of ERK and AKT signaling pathways associated with upregulation of cyclin D1 and downregulation of p16, Stem Cells Dev. 26 (2017) 113–122, https://doi.org/10.1089/scd.2016.0234.
[24] P. Mistriotis, S.T. Andreadis, Hair follicle: a novel source of multipotent stem cells for tissue engineering and regenerative medicine, Tissue Eng. Part B Rev. 19 (2013) 265–278, https://doi.org/10.1089/ten.TEB.2012.0422.
[25] M. Iida, S. Ihara, T. Matsuzaki, Hair cycle-dependent changes of alkaline phosphatase activity in the mesenchyme and epithelium in mouse vibrissal follicles, Develop. Growth Differ. 49 (2007) 185–195, https://doi.org/10.1111/j.1440-169X.2007.00907.x.
[26] R.R. Driskell, C. Clavel, M. Rendl, F.M. Watt, Hair follicle dermal papilla cells at a glance, J. Cell Sci. 124 (2011) 1179–1182, https://doi.org/10.1242/jcs.082446.
[27] M. Wegner, C.C. Stolt, From stem cells to neurons and glia: a Soxist's view of neural development, Trends Neurosci. 28 (2005) 583–588, https://doi.org/10.1016/j.tins.2005.08.008.
[28] M.J. Hoogduijn, E. Gorjup, P.G. Genever, Comparative characterization of hair follicle dermal stem cells and bone marrow mesenchymal stem cells, Stem Cells Dev. 15 (2006) 49–60, https://doi.org/10.1089/scd.2006.15.49.
[29] S. Ma, N. Xie, W. Li, B. Yuan, Y. Shi, Y. Wang, Immunobiology of mesenchymal stem cells, Cell Death Differ. 21 (2014) 216–225, https://doi.org/10.1038/cdd.2013.158.
[30] R.M. Boehler, R. Kuo, S. Shin, A.G. Goodman, M.A. Pilecki, R.M. Gower, J.N. Leonard, L.D. Shea, Lentivirus delivery of IL-10 to promote and sustain macrophage polarization towards an anti-inflammatory phenotype, Biotechnol. Bioeng. 111 (2014) 1210–1221, https://doi.org/10.1038/cdd.2013.158.
[31] F. Zhang, H. Wang, X. Wang, G. Jiang, H. Liu, G. Zhang, H. Wang, R. Fang, X. Bu, S. Cai, J. Du, TGF-β induces M2-like macrophage polarization via SNAIL-mediated suppression of a pro-inflammatory phenotype, Oncotarget 7 (2016) 52294–52306, https://doi.org/10.18632/oncotarget.10561.
[32] X. Kong, J. Gao, Macrophage polarization: a key event in the secondary phase of acute spinal cord injury, J. Cell. Mol. Med. 21 (2017) 941–954, https://doi.org/10.1111/jcmm.13034.
[33] M. Song, K. Martinowich, F.S. Lee, BDNF at the synapse: why location matters, Mol. Psychiatry 22 (2017) 1370–1375, https://doi.org/10.1038/mp.2017.144.
[34] E.D. Papathanassoglou, P. Miltiadous, M.N. Karanikola, May BDNF be implicated in the exercise-mediated regulation of inflammation? Critical review and synthesis of evidence, Biol. Res. Nurs. 17 (2015) 521–539, https://doi.org/10.1177/1099800414555411.
[35] E. Vergadi, E. Ieronymaki, K. Lyroni, K. Vaporidi, C. Tsatsanis, Akt signaling pathway in macrophage activation and M1/M2 polarization, J. Immunol. 198 (2017) 1006–1014, https://doi.org/10.4049/jimmunol.1601515.
[36] A. Arranz, C. Doxaki, E. Vergadi, Y. Martinez De La Torre, K. Vaporidi, E.D. Lagoudaki, E. Ieronymaki, A. Androulidaki, M. Venihaki, A.N. Margioris, E.N. Stathopoulos, P.N. Tsichlis, C. Tsatsanis, Akt1 and Akt2 protein kinases differentially contribute to macrophage polarization, Proc. Nat. Acad. Sci. U. S. A. 109 (2012) 9517–9522, https://doi.org/10.1073/pnas.1119038109.
[37] X. Shi, X. Cai, W. Di, J. Li, X. Xu, A. Zhang, W. Qi, Z. Zhou, Y. Fang, MFG-E8 selectively inhibited Aβ-induced microglial M1 polarization via NF-κB and PI3K-Akt pathways, Mol. Neurobiol. 54 (2017) 7777–7788, https://doi.org/10.1007/s12035-016-0255-y.